# The $I_{Ks}$ ion channel activator, mefenamic acid, requires KCNE1 and modulates channel gating in a subunit-dependent manner

Yundi Wang, Jodene Eldstrom, and David Fedida[*]

Department of Anesthesiology, Pharmacology and Therapeutics, University of British Columbia,

Vancouver, British Columbia, Canada

Keywords: $I_{Ks}$, mefenamic acid, KCNE1, KCNQ1, single channels, gating modifier

1

# Mefenamic acid activates $I_{Ks}$ gating in a subunit-dependent manner

\* Corresponding author: **Dr. David Fedida**

Life Sciences Centre, 2350 Health Sciences Mall, Room 2.301 Vancouver, British Columbia,

Canada V6T 1Z3

Telephone: +1 (604) 822-5806, Email: david.fedida@ubc.ca

Number of Text Pages: 45

Number of Tables: 2

Number of Figures: 8 (+ 1 Supplemental Figure)

Number of References: 40

Number of Words in Abstract: 246

Number of Words in Introduction: 701

Number of Words in Methods: 1449

Number of Words in Results: 2964

Number of Words in Discussion: 2140

## Abbreviations

$I_{Ks}$; delayed cardiac rectifier $K^+$ current, LQTS; long QT syndrome, PBA; phenylboronic acid,

HCP; hexachlorophene, DIDS; 4,4'-diisothiocyano-2,2'-stilbenedisulfonic acid, SITS; 4-

acetamido-4'-isothiocyanatostilbene-2,2'-disulfonic acid, HMR1556; (3R,4S)-(+)-N-[3-hydroxy-

2,2-dimethyl-6-(4,4,4-trifluorobutoxy) chroman-4-yl]-N-methylmethanesulfonamide, LM; *ltk*-

mouse fibroblast cells, $EC_{50}$; half maximal effective concentration; $n^H$; hill coefficient, $I_{max}$ - $I_{min}$;

peak to steady state difference currents, $I_{min}$; minimum current amplitude, $I_{max}$; peak current amplitude, I-V; current-voltage relationship, G-V; conductance-voltage relationship, $k$; slope factor, $V_{1/2}$; voltage at half-maximal activation, WT; wild type, $EC_{max}$; maximal effective concentration

## Abstract

The pairing of KCNQ1 and KCNE1 subunits together mediates the cardiac slow delayed rectifier current ($I_{Ks}$), which is partly responsible for cardiomyocyte repolarization and physiological shortening of the cardiac action potential. Mefenamic acid, an NSAID, has been identified as an $I_{Ks}$ activator. Here, we provide a biophysical and pharmacological characterization of mefenamic acid's effect on $I_{Ks}$. Using whole-cell patch-clamp, we show that mefenamic acid enhances $I_{Ks}$ activity in both a dose- and stoichiometry-dependent fashion by changing the slowly activating and deactivating $I_{Ks}$ current into an almost linear current with instantaneous onset and slowed tail current decay, all of which are sensitive to the $I_{Ks}$ blocker, HMR1556. Both single channels, which reveal no change in the maximum conductance, and whole-cell studies which reveal a dramatically altered G-V relationship despite increasingly longer interpulse intervals, suggest mefenamic acid decreases the voltage sensitivity of the $I_{Ks}$ channel, and shifts channel gating kinetics towards more negative potentials. Modeling studies revealed that changes in voltage sensor activation kinetics are sufficient to reproduce the dose- and frequency-dependence of mefenamic acid action on $I_{Ks}$ channels. Mutational analysis showed that mefenamic acid's effect on $I_{Ks}$ required residue K41 and potentially other surrounding residues on the extracellular surface of KCNE1, and explains why the KCNQ1 channel alone is insensitive to up to 1 mM mefenamic acid. Given that mefenamic acid can enhance all $I_{Ks}$ channel complexes containing different ratios of KCNQ1 to KCNE1, it may provide a promising therapeutic approach to treating life-threatening cardiac arrhythmia syndromes.

## Significance Statement

The channels which generate the $I_{Ks}$ current are composed of KCNQ1 and KCNE1 subunits. Due to the critical role played by $I_{Ks}$ in heartbeat regulation, enhancing $I_{Ks}$ current has been identified as a promising therapeutic strategy to treat various heart rhythm diseases. Most $I_{Ks}$ activators unfortunately, only work on KCNQ1 alone and not the physiologically relevant $I_{Ks}$ channel. We have demonstrated that mefenamic acid can enhance $I_{Ks}$ in a dose- and stoichiometry-dependent fashion, regulated by its interactions with KCNE1.

**Introduction**

The potassium voltage-gated KCNQ channel subfamily is comprised of five known isoforms, KCNQ1-5 (Abbott, 2014). Expression of the first isoform, KCNQ1, has been detected throughout the body including in the heart, stomach and ear (Liin et al., 2015). When by itself, KCNQ1 produces a fast activating and deactivating current that has not yet been found to underlie any specific endogenous currents in the body (Abbott, 2014). KCNQ1 however, also co-assembles with several β-subunits, KCNE1-5, which modulate KCNQ1 current kinetics (Bendahhou et al., 2005; Manderfield and George, 2008; Eldstrom and Fedida, 2011). In the heart, the co-assembly of KCNQ1 with KCNE1 and perhaps other KCNE subunits, produces a slowly activating and deactivating delayed cardiac rectifier K$^+$ current ($I_{Ks}$), which contributes significantly to cardiac repolarization (Sanguinetti et al., 1996; Lundquist et al., 2005).

There is no general agreement on the stoichiometric ratio of KCNE1 to KCNQ1 subunits underlying $I_{Ks}$, either *in vivo*, or in heterologous *in vitro* expression systems (Morin and Kobertz, 2008; Nakajo et al., 2010; Plant et al., 2014; Murray et al., 2016), though we know a variable stoichiometry of 4:1 up to 4:4 is possible (Murray et al., 2016). Given that the kinetics of $I_{Ks}$ are greatly affected by the number of KCNE1 subunits, great flexibility in the expressed physiological and pharmacological properties of $I_{Ks}$ channel complexes is expected from a variable stoichiometry.

The complex also has clinical importance in disease syndromes including cardiac arrhythmia, with the severity ranging from syncope to sudden death (Splawski et al., 2000). Approximately 50% of the mutations seen in long QT syndrome (LQTS) patients are in the KCNQ1 subunit (LQTS type 1) (Hedley et al., 2009), with mutations in KCNE1 causing LQTS type 5.

Activators of $I_{Ks}$ that can act on the relevant saturated and unsaturated $I_{Ks}$ complexes are of particular interest as they may have therapeutic potential in the treatment of LQTS types 1 and 5. To date, although several activators have been reported, some are only effective on KCNQ1 alone with limited efficacy on $I_{Ks}$. These include ML-277, zinc pyrithione and L-364,373 (Magyar et al., 2006; Gao et al., 2008; Yu et al., 2013). The known activators of $I_{Ks}$ are phenylboronic acid (PBA) (Mruk and Kobertz, 2009) and hexachlorophene (HCP) (Zheng et al., 2012), as well as stilbenes such as 4,4'-diisothiocyano-2,2'-stilbenedisulfonic acid (DIDS) and 4-acetamido-4'-isothiocyanatostilbene-2,2'-disulfonic acid (SITS), fenamates such as mefenamic acid (Abitbol et al., 1999), and fatty acids such as lauric acid (Doolan et al., 2002). PBA and HCP have been shown to increase both KCNQ1 alone and $I_{Ks}$ current amplitudes, although they are more potent on $I_{Ks}$ (Mruk and Kobertz, 2009; Zheng et al., 2012). In contrast, lauric acid, DIDS and SITS have been shown to only increase $I_{Ks}$ current (Abitbol et al., 1999; Doolan et al., 2002).

The fenamate, mefenamic acid (Fig. 1A), is a nonsteroidal anti-inflammatory drug primarily prescribed to treat menstrual pains (U.S. FDA, 2008). Originally identified as a chloride channel blocker, mefenamic acid has since been shown in various expression systems (*Xenopus* oocytes, rat mesenteric arteries, canine ventricular myocytes, guinea-pig ventricular myocytes, CHO cells and COS-7 cells) to increase mammalian $I_{Ks}$ current amplitudes as well as produce a variable amount of instantaneous current and inhibit tail current decay (Busch et al., 1994; Abitbol et al., 1999; Unsöld et al., 2000; Magyar et al., 2006; Toyoda et al., 2006; Chadha et al., 2012).

In the present study, using transiently expressed human $I_{Ks}$ in mammalian cells, we have carried out a more complete biophysical characterization of the effects of mefenamic acid than has been attempted to date. We show that mefenamic acid has minimal effect on KCNQ1 in the absence of

KCNE1 and have quantified drug concentration- and rate-dependent changes in the $I_{Ks}$ current

waveforms, the conductance-voltage relationship, and single channel conductance and kinetics.

As the stoichiometry of $I_{Ks}$ may vary and affect its pharmacology and current kinetics (Nakajo et

al., 2010; Murray et al., 2016), we have analyzed the dependence of mefenamic acid actions on

the stoichiometry of $I_{Ks}$ channel complexes. Lastly, through mutational analysis we identify a

specific regulatory site for mefenamic acid on KCNE1. The results suggest that residue K41 on

KCNE1 is of particular importance in mediating the effect mefenamic acid has on $I_{Ks}$.

## Materials and Methods

### Solutions and Drugs

Unless otherwise stated, all drugs and chemicals used to make solutions were obtained from Sigma-Aldrich (Mississauga, ON, Canada). The control bath solution for whole-cell experiments contained: 135 mM NaCl, 5 mM KCl, 1 mM $MgCl_2$, 2.8 mM NaAcetate and 10 mM HEPES, pH 7.4 with NaOH. The pipette solution for whole-cell experiments contained: 130 mM KCl, 5 mM EGTA, 1 mM $MgCl_2$, 4 mM $Na_2$-ATP, 0.1 mM GTP and 10 mM HEPES, pH 7.2 with KOH. The control bath solution for single channel experiments contained: 135 mM KCl, 1 mM $MgCl_2$, 50 µM $CaCl_2$, 10 mM Dextrose, 10 mM HEPES, pH 7.4 with KOH. The pipette solution for single channel experiments contained: 6 mM NaCl, 129 mM MES, 1 mM $MgCl_2$, 5 mM KCl, 10 mM HEPES, pH 7.4 with NaOH. Mefenamic acid and HMR1556 ((3R,4S)-(+)-N-[3-hydroxy-2,2-dimethyl-6-(4,4,4-trifluorobutoxy) chroman-4-yl]-N-methylmethanesulfonamide) (Tocris Bioscience, Oakville, ON, Canada) were prepared as stock solutions (50 mM, 200 mM or 500 mM for mefenamic acid and, 2 mM for HMR1556) dissolved in 100% dimethyl sulfoxide. Stock mefenamic acid solutions were diluted in control whole-cell bath solution to obtain final mefenamic acid concentrations of 10 µM, 30 µM, 100 µM, 300 µM, 500 µM or 1 mM which were perfused onto mammalian cells for whole-cell experiments. Stock HMR1556 and mefenamic acid solutions were pipetted directly into the chamber to obtain a final HMR1556 concentration of 1 µM for whole-cell experiments or, a final mefenamic acid concentration of 100 µM for single channel experiments. Concentrations of dimethyl sulfoxide in final bath solutions never exceeded 0.2% (V/V). The maximum concentration of mefenamic acid (1 mM) lowered the pH of the final bath solution by $0.15 \pm 0.02$ (n=3). This was not corrected.

**Constructs, Cell Culture and Transfection**

$I_{Ks}$ is generally understood to be functionally comprised of combinations of KCNQ1 and KCNE1 subunits. The stoichiometry of the two subunits may be variable in heterologous expression systems (Murray et al., 2016), and may also vary *in-vivo* (Dvir et al., 2014). In the initial experiments (Figs. 1-4), the initial stoichiometric ratio of KCNQ1:KCNE1 was set at the maximum, 4:4. This was achieved through transfection of a linked KCNE1 and KCNQ1 cDNA (Murray et al., 2016), which is expected to assemble as a tetramer with four KCNQ1 and four KCNE1 subunits. For simplicity this will be denoted as EQ. In later experiments where the ratio was varied (Fig. 5), cells were transfected with KCNQ1 without KCNE1 (Q1), or linked constructs containing one KCNE1 linked with two KCNQ1s (EQQ, expected to assemble in a 2:4 ratio), or one KCNE1 linked with four KCNQ1s (EQQQQ, expected to assemble in a 1:4 ratio). EQ, EQQ and EQQQQ constructs were generated as previously described (Murray et al., 2016). In all cases we consider the currents that result from different combinations of KCNQ1 and KCNE1 (except KCNQ1 alone, Q1) to be $I_{Ks}$ and we use this name interchangeably with the constructs themselves.

tsA201 transformed human embryonic kidney 293 or *ltk-* mouse fibroblast cells were cultured in modified Eagle's medium supplemented with 10% fetal calf serum and 100 µg/mL penicillin, 100 µg/mL streptomycin and 0.25 µg/mL amphotericin and, plated for whole-cell and single channel experiments as previously described (Murray et al., 2016; Westhoff et al., 2019). Cells were transiently transfected with either: 1) GFP tagged Q1 (Q1-GFP); 2) EQ, EQQ or EQQQQ and GFP in a 1.5-2.5:1.0 µg ratio or; 3) mutant KCNE1 and Q1-GFP in a 4.5-6.0:1.5 µg ratio using Lipofectamine2000 (Thermo Fisher Scientific, Waltham, MA, USA) as per the manufacturer's protocol. All KCNE1 mutations were generated using site-directed mutagenesis and Pfu Turbo

(Agilent Technologies, Santa Clara, CA, USA) followed by sequence confirmation of all mutations. Whole-cell and single channel experiments were conducted 24 to 48 hrs post transfection.

**Electrophysiology**

An Axopatch 200B amplifier, Digidata 1440A (whole-cell experiments) or Digidata 1322A (single channel experiments) and pClamp 9 or 11 software was used to conduct all experiments. For whole-cell experiments, electrodes ranging from 1-3 MΩ resistance were first pulled from thin-walled borosilicate glass (Sutter Instruments, Cal. USA) using a linear multistage electrode puller (Sutter Instruments) and then fire polished before use. Series resistance compensation of 70-80% was used for all whole-cell experiments. Data were sampled at 20 kHz and filtered at 5 kHz during acquisition. Electrodes for single channel experiments were pulled from thick-walled borosilicate glass (Sutter Instruments) and fire polished to resistances between 40 and 60 MΩ. Before recording, electrodes were coated with Sylgard (Dow Corning, Midland, MI, USA). Current records were sampled at 10 kHz, low-pass filtered at 2 kHz at acquisition using a −3dB, four-pole Bessel filter, and digitally filtered at 200 Hz for presentation and analysis (Werry et al., 2013; Eldstrom et al., 2015; Murray et al., 2016; Thompson et al., 2017; Westhoff et al., 2017). For voltage clamp protocols, interpulse intervals refer to start-to-start times between sweeps.

**Data analysis**

GraphPad Prism 8.1.1 software was used to analyze all data. Where applicable, One-way Anova followed by the Bonferroni multiple comparison post-hoc test was used to determine statistical

significance. A p-value less than 0.05 was considered statistically significant. All data in the

figures are shown as mean ± SEM and reported in the tables as mean ± SD.

*Whole-cell experiments:* Mefenamic acid dose-response diary plots (Figs. 1B-C right panels) and

curves (Figs. 2A-B and 5D) were obtained from measurement of the activating $I_{Ks}$ current.

Specifically, the peak to steady state difference currents ($I_{max} - I_{min}$) were calculated by subtracting

the minimum amplitude of the activating current ($I_{min}$) from the peak amplitude of the activating

current ($I_{max}$). This value was then plotted against either the corresponding sweep number or $\log_{10}$

concentration of mefenamic acid (Figs. 1 and 2A). Where applicable, the difference current in

mefenamic acid was normalized to the maximum control (in the absence of mefenamic acid)

difference current, and subtracted from 1.0 to obtain the 'Normalized Response', which was

plotted against the corresponding $\log_{10}$ concentration of mefenamic acid (Figs. 2B, 5D, and 8B).

Dose- and Normalized-response curves were fit with a specific binding equation in order to obtain

the $EC_{50}$ and Hill coefficients ($n^H$) as in Figures 2A-B, 5D and 8B. The HMR1556 response diary

plot in the presence of mefenamic acid (Fig. 1D right panel) was obtained by plotting the initial

peak current amplitude against the corresponding sweep number. All current-voltage (I-V) and

conductance-voltage (G-V) plots in Figures 3, 5 and 7 and Supplemental Figure 1 were obtained

from the normalized peak of the 4 s depolarizing pulses ($I/I_{max}$) and normalized peak of the initial

tail current ($G/G_{max}$), respectively, and plotted against the corresponding voltage. G-V plots were

fitted with a Boltzmann sigmoid equation in order to obtain the $V_{1/2}$ and slope ($k$) values (Tables 1

and 2). In the case of the mutant EQ $I_{Ks}$, the change in $V_{1/2}$ of activation ($\Delta V_{1/2} = V_{1/2}$ in the presence

of mefenamic acid $- V_{1/2}$ control) was further determined (Fig. 7D; Table 2). In some cells, G-V

relationships in the presence of mefenamic acid for WT EQ, K41R and G40C were essentially

12

linear, and consequently the $V_{1/2}$ of activation was read from the plots and included in the calculations of the mean values in Tables 1 and 2. All deactivation traces in Figures 4A-B were fitted with a single exponential equation in order to obtain the time constants of deactivation ($\tau_{deact}$) which were plotted against the corresponding membrane potential (Fig. 4C).

## Modeling

Markov modeling in Figure 8 was carried out using the IonChannelLab software (Santiago-Castillo et al., 2010) incorporating Q-matrix solutions to the differential equations defining the kinetic behavior of rate transitions (Colquhoun and Hawkes, 1995). A balanced model (Zaydman et al., 2014) as revised by Westhoff et al. (Westhoff et al., 2019) was used for simulations, using a 4:4 KCNQ1:KCNE1 stoichiometry. In this model each voltage sensor (VS) is assumed to undergo two activating transitions, to an intermediate and then activated conformation. Pore subconductance opening can occur as soon as each VS is fully activated, and thus pore opening does not require a concerted step after all four VS have reached fully activated conformations. For full model exposition and rates, see Westhoff et al. 2019. In order to simulate the action of mefenamic acid on $I_{Ks}$ currents, the intrinsic rates of forward VS transitions at 0 mV, between resting and intermediate states ($k_{RI}0$) and between intermediate and activated states ($k_{IA}$) were multiplied by the drug concentration (D, in μM), or $\log_{10}$ [D], respectively. This difference reflected the fact that an extreme hyperpolarization of the G-V relation, and facilitation of initial steps of activation were caused by mefenamic acid at higher concentrations or rates of activation (Fig. 3), and thus a greater acceleration of the first VS transition was required to simulate experimental data.

### Results

**Mefenamic acid increases EQ $I_{Ks}$ current expressed in mammalian cells.**

Initially, to ensure that mefenamic acid (Fig. 1A) had no effect on the endogenous currents in *ltk*-mouse fibroblast (LM) cells, different concentrations of mefenamic acid (10 µM, 30 µM, 100 µM 300 µM, 500 µM and 1 mM) were perfused onto untransfected LM cells (Fig. 1B). At all concentrations of mefenamic acid, no changes were observed in the waveform (Fig. 1B left panel) and peak to steady-state difference currents ($I_{max}$ - $I_{min}$; Fig. 1B right panel) compared to untreated cells (control). A single concentration of mefenamic acid (100 µM) has previously been shown to enhance $I_{Ks}$ activity leading to a variable amount of instantaneous current and inhibition of tail current decay in *Xenopus* oocytes (Busch et al., 1994; Busch et al., 1997) and various mammalian cells (Unsöld et al., 2000; Magyar et al., 2006; Toyoda et al., 2006). The concentration dependence of this enhancement of $I_{Ks}$ activity using different concentrations of mefenamic acid perfused onto LM cells transiently transfected with EQ is shown in Figure 1C. With increasing concentrations of mefenamic acid, the control sigmoidal waveform (indicative of slow activation kinetics), was transformed into an almost linear waveform with significant instantaneous current (Fig. 1C left panel). The corresponding difference current diary plot of increasing concentrations of mefenamic acid shows the gradual transformation to an instantaneous current over time (Fig. 1C right panel). Consistent with previous findings, the decay in tail current seen in control was also inhibited in a dose-dependent manner with increasing concentrations of mefenamic acid (Fig. 1C left panel).

To confirm that this instantaneous current was produced by mefenamic acid enhancement of $I_{Ks}$ activity specifically, we employed the $I_{Ks}$ blocker, HMR1556 (Gögelein et al., 2000). In these experiments, LM cells transiently transfected with EQ were first preincubated in 100 µM

14

mefenamic acid for approximately 30 min (data not shown), then when an $I_{Ks}$-positive cell was identified, 1 µM HMR1556, was applied to the bath (Fig. 1D). As is evident in the representative traces (Fig. 1D left panel) and diary plot (Fig. 1D right panel), following HMR1556 treatment, the instantaneous current amplitude decreased over time to that of endogenous current amplitudes, suggesting that the instantaneous current was in fact flowing through $I_{Ks}$ channels.

**Mefenamic acid dose-response curves for EQ $I_{Ks}$.**

Increasing concentrations of mefenamic acid gradually transformed the sigmoidal activation waveform of EQ $I_{Ks}$ into an almost linear waveform, and this change was quantified by measuring peak to steady-state difference currents (Fig. 2A upper panel; see Methods). More specifically, difference currents were calculated by subtracting the initial amplitude of the activating current ($I_{min}$) from the peak amplitude of the activating current ($I_{max}$) and plotting it against the corresponding log concentration of mefenamic acid (Fig. 2A). Normalized Response relationships for EQ were obtained by transformation of $I_{max}$-$I_{min}$ data (see Methods) and fit with a specific binding equation (Fig. 2B). The $EC_{50}$ and Hill Coefficient ($n^H$) for mefenamic acid were 60 µM and 0.49, respectively. To ensure consistent results and to allow for comparison with previous literature, all subsequent experiments to characterize the gating properties, the subunit stoichiometry, and specific regulatory residues were conducted using 100 µM mefenamic acid, unless otherwise stated.

**Mefenamic acid rate-dependently hyperpolarizes EQ $I_{Ks}$ I-V and G-V relationships.**

To investigate what happens to EQ $I_{Ks}$ I-V and G-V relationships following treatment with 100 µM mefenamic acid, a 4 s activation protocol with varying interpulse intervals was used (Fig. 3).

In Figure 3A are representative waveforms of EQ $I_{Ks}$ both in the absence (control; upper panel) and presence of mefenamic acid (lower panel) and, show the characteristic delay of current activation in control and the appearance of an instantaneous current with mefenamic acid treatment. The corresponding I-V (Fig. 3B) and G-V relationships (Fig. 3C) were obtained by plotting the normalized peak amplitudes at the end of the 4 s depolarizing pulses ($I/I_{max}$) or the normalized peak of the initial tail current ($G/G_{max}$), respectively, against the corresponding voltage. During exposure to mefenamic acid, the I-V relationship became more linear and hyperpolarized (Fig. 3B). The G-V relationship following treatment with mefenamic acid was also hyperpolarized (control: $V_{1/2} = 24.0$ mV; $k = 24.0$ mV; mefenamic acid: $V_{1/2} = -2.4$ mV; $k = 65.4$ mV; Fig. 3C).

Visually, all the I-V relationships at different interpulse intervals (30 s, 20 s, 15 s and 7 s) in the presence of mefenamic acid appeared almost linear and more hyperpolarized (Fig. 3D). The degree of hyperpolarization was graded with increasingly shorter intervals and I-V relationships for interpulse intervals of 7 s and 30 s were respectively, the most and least hyperpolarized. In contrast, altering the interpulse interval dramatically affected the G-V relationships of mefenamic acid-treated EQ (Fig. 3E). The degree of hyperpolarization of the G-V plots and $V_{1/2}$ of activation was also greater with shorter interpulse intervals. The G-V relationship and $V_{1/2}$ for an interpulse interval of 7 s (-108 mV) was the most hyperpolarized followed by the G-Vs and $V_{1/2}$s at interpulse intervals of 15 s (-86.5 mV), 20 s (-80.5 mV) and, finally, 30 s (-13.1 mV) which was the least hyperpolarized (Table 1). The $V_{1/2}$ of activation at all tested interpulse intervals (30 s, 20 s, 15 s and 7s) in the presence of mefenamic acid was significantly different from control (Table 1). The slope of the G-V relationship was significantly decreased when the interpulse interval was either 20 s (53.3 mV; $p = 0.0045$) or 30 s (57.2 mV; $p = 0.0035$) in the presence of mefenamic acid when

16

compared to control (20.4 mV) (Table 1). The slope of the G-V relationship, however, was not significantly different when the interpulse interval was 15 s (23.2 mV) or 7 s (6.9 mV) in the presence of mefenamic acid when compared to control (Table 1).

Altering the interpulse interval of the activation protocol to 7 s however, did not significantly affect the control (in the absence of mefenamic acid) I-V and G-V relationships (Figs. 3D-E), although the G-V relationship did become steeper. Overall, these results show that mefenamic acid hyperpolarizes the I-V and G-V relationships of EQ $I_{Ks}$ in a rate-dependent fashion.

**Mefenamic acid slows EQ $I_{Ks}$ deactivation.**

To investigate changes in rates of EQ deactivation following treatment with 100 µM mefenamic acid, tail currents were obtained in the absence (Fig. 4A) and presence of mefenamic acid (Fig. 4B) and fit with single exponential decay curves. Deactivation time constants were obtained from these fits and plotted against the membrane potential (Fig. 4C). The $K^+$ reversal potential was found to be approximately -80 mV, and therefore the rate of deactivation at -80 mV was omitted. Treatment with mefenamic acid significantly decreased the rate of deactivation at -70 to -140 mV.

**Effect of $I_{Ks}$ stoichiometry on response to 100 µM mefenamic acid.**

To investigate whether the effect of mefenamic acid on $I_{Ks}$ dose-response and G-V relationships was dependent on the E1:Q1 stoichiometry, mammalian cells (LM and tsA201 cells) were transiently transfected with either EQ $I_{Ks}$, EQQ $I_{Ks}$, EQQQQ $I_{Ks}$ or KCNQ1 alone (Fig. 5). These $I_{Ks}$ constructs fix the ratio of E1:Q1 to either 4:4, 2:4 or 1:4 through linking the C-terminus of KCNE1 to the N-terminus of one, two or four KCNQ1 sequences, respectively.

17

No change in the KCNQ1 waveform was seen following treatment with 100 µM mefenamic acid
(control: Fig. 5A left upper panel; mefenamic acid: Fig. 5A left lower panel). Mefenamic acid also
did not significantly shift the $V_{1/2}$ of activation or slope of the G-V relationship (Table 2),
supporting the conclusion that mefenamic acid has no effect on KCNQ1 alone.

When one KCNE1 subunit was present (EQQQQ $I_{Ks}$), the instantaneous current characteristic of
mefenamic acid's effect on EQ $I_{Ks}$ no longer occurred (Fig. 5B left panel). The EQQQQ $I_{Ks}$
waveform was sigmoidal both in the absence (Fig. 5A left upper panel) and presence of 100 µM
mefenamic acid (Fig. 5A left lower panel). Despite mefenamic acid not having a dramatic
transformative effect on the activation waveform of EQQQQ, inhibition of EQQQQ tail current
decay following mefenamic acid treatment still occurred. A significant leftward shift in the $V_{1/2}$ of
activation also occurred (control: -1.5 mV; mefenamic acid: -20.8 mV; p = 0.0298; Table 2). There
were no significant changes in the slope of the G-V relationships.

Similar to EQQQQ $I_{Ks}$, there was no dramatic transformative effect on the EQQ $I_{Ks}$ activation
waveform following mefenamic acid treatment (Fig. 5C left panel). Inhibition of EQQ $I_{Ks}$ tail
current decay however, still occurred. A significant leftward shift in the $V_{1/2}$ of activation also
occurred (control: 15.4 mV; mefenamic acid: -1.6 mV; p = 0.0472; Table 2). Again, the slope of
the G-V relationships did not change. Overall, the leftward shift in the $V_{1/2}$ of activation ($\Delta V_{1/2}$)
for EQQQQ (-19.3 mV) and EQQ (-17.1mV) was less dramatic than the $\Delta V_{1/2}$ of activation for
EQ (-110 mV) (Table 2). The normalized responses of the different $I_{Ks}$ stoichiometries (normalized
difference currents) to different concentrations of mefenamic acid are plotted in Figure 5D. At all
concentrations, the normalized responses of EQQQQ $I_{Ks}$ and EQQ $I_{Ks}$ were significantly reduced

18

compared to the response of EQ $I_{Ks}$. The EC$_{50}$ and $n^H$ were, respectively: 902 µM and 0.66 for

EQQQQ $I_{Ks}$; 615 µM and 0.47 for EQQ $I_{Ks}$; and, 60 µM and 0.49 for EQ $I_{Ks}$. Since no change in

the KCNQ1 waveform or significant shift in the V$_{1/2}$ was seen following mefenamic acid treatment

(Fig. 5A), these data were not included in the log concentration-Normalized Response plot in

Figure 5D.


**Mefenamic acid effects at the single channel level.**

In order to determine if the enhancement of $I_{Ks}$ current upon mefenamic acid treatment was a result

simply of an increase in open probability or there were additional effects on conductance, we made

single channel recordings of 4:4 $I_{Ks}$ stoichiometry (EQ) in the presence of the drug. Figure 6A

shows three representative active traces of control EQ and three in the presence of 100 µM

mefenamic acid. The voltage protocol was analogous to the whole cell experiments in that a 4 s

depolarization was given, with a 0.75 s repolarization period at -40 mV, applied every 10 s.


It is clear from these records that channels opened very early upon depolarization in the presence

of mefenamic acid (Fig. 6A, bottom three sweeps), and that channel openings were persistent

during the repolarization step to -40 mV. Thus, first latency was shortened and deactivation slowed

in the presence of mefenamic acid, as would be expected based on the whole-cell recordings. Note

that, during exposure to mefenamic acid, channels were not already activated when initially

depolarized as might have been expected if the effects of mefenamic acid were simply related to a

failure of deactivation between pulses. It is clear that channels activate *de novo* with each pulse.

This is confirmed in the ensemble averages of 18 active sweeps of control and 18 sweeps from the

same recording taken approximately 23 min after mefenamic acid exposure (Fig. 6B) where

channel activity was seen earlier during the depolarization in the presence of mefenamic acid (red

tracing) than in control (blue tracing), and tail currents persisted to the end of the recording period.

The all-points histograms (Fig. 6C) comparing events in the three control and three mefenamic

acid sweeps shown in Figure 6A also show a reduction in the number of closed events, which is

indicative of increased channel activity and decreased latency in the presence of mefenamic acid.

In addition, the peak open amplitude around 0.4 pA is maintained, but shows more events due to

prolonged opening bursts seen in the presence of mefenamic acid. Maximum channel conductance

was not increased by mefenamic acid, it is rather that simply more open events were seen at the

same levels present in control.


Another important observation from the single channel experiments using the cell attached

configuration was the delay in action of mefenamic acid.  In whole-cell experiments, mefenamic

acid effects were observed within approximately 0.5-1 min of bath application, whereas when the

extracellular domain of $I_{Ks}$ was shielded by the recording electrode in the cell-attached

configuration, the effect took up to 20 min to become obvious. This supports previous research

pointing to an extracellular binding site for the drug (Abitbol et al., 1999). When mefenamic acid

was included in the patch pipette, the effect on open probability was fairly immediate (data not

shown).


**Mapping the mefenamic acid regulatory sites on KCNE1.**

Since our data indicate that mefenamic acid has minimal effect on KCNQ1 alone and the effect of

mefenamic acid is dependent upon channel stoichiometry, we further examined potential

mefenamic acid regulatory sites on KCNE1. The binding site for mefenamic acid has previously

been suggested to lie between residues 39-43 on KCNE1 (Abitbol et al., 1999), however, the importance of each residue to mefenamic acid's subsequent effect on $I_{Ks}$ have not previously been characterized. Using mutational analysis, we therefore characterized how singularly mutating residues in this region would affect mefenamic acid's ability to alter the waveform and G-V relationship of EQ $I_{Ks}$.

Similar to WT EQ $I_{Ks}$, all mutant EQ $I_{Ks}$ showed the characteristic delay of current activation in the absence of mefenamic acid (L42C, Fig. 7A; K41C, Fig. 7B; K41R, Fig. 7C; G40C, Supplemental Fig. 1A; current data not shown for K41E and E43C). Additionally, the characteristic appearance of instantaneous current and inhibition of tail current decay induced by mefenamic acid on WT EQ $I_{Ks}$ was preserved in the G40C (Supplemental Fig. 1B), L42C (Fig. 7A) and E43C (data not shown) EQ $I_{Ks}$ mutants. When an interpulse interval of 15 s was used, mefenamic acid also significantly altered the shape of the G-V relationship (Supplemental Fig. 1C) and left shifted the $V_{1/2}$ of activation for G40C ($\Delta V_{1/2}$: -76.1 mV) (Table 2, Fig. 7D). This effect on the G-V relationship and $V_{1/2}$ of G40C was also dependent on the interpulse interval – with the shortest interpulse interval (interpulse intervals examined include: 7 s, 15 s and 30 s) producing the most dramatically altered G-V relationship (Supplemental Fig. 1C) and visually the most leftward shift in $V_{1/2}$. In contrast, the effect mefenamic acid had on the G-V relationships of L42C and E43C were not as dramatic (L42C: Fig. 7A right panel; data not shown for E43C). When an interpulse interval of 15 s was used, the shape of the G-V relationship in both the absence and presence of mefenamic acid was sigmoidal for L42C and E43C. As well, the slope of the G-V relationship was not significantly altered following mefenamic acid treatment, however a significant hyperpolarizing shift in the $V_{1/2}$ of activation occurred ($\Delta V_{1/2}$ for L42C: -37.2 mV;

21

$\Delta V_{1/2}$ for E43C: -24.4 mV) (Table 2, Fig. 7D) for both mutants. Mutating residues L42, E43 and, especially G40 on KCNE1 therefore only minimally reduced mefenamic acid's effect on EQ $I_{Ks}$.

Mutations made at K41 on KCNE1 had a different result. Unlike WT EQ $I_{Ks}$, after treatment with 100 μM mefenamic acid, the waveform of K41C still showed delayed current activation and WT tail current decay (Fig. 7B lower left panel). Moreover, there was also no change in the slope and shape of the G-V relationship, (Fig. 7B right panel) or significant shift in the $V_{1/2}$ of activation (Table 2, Fig. 7D). Even in the presence of 1 mM mefenamic acid, there was still no effect on the slope and shape of the G-V relationship (Fig. 7B right panel) or significant shift in the $V_{1/2}$ of activation when compared to control (Table 2, Fig. 7D). Mutating residue K41 therefore drastically reduced mefenamic acid's effect on EQ $I_{Ks}$. We hypothesized that neutralization of the positively charged K41 was responsible for the loss of efficacy of mefenamic acid. In support of this idea, similar to K41C, after treatment with 100 μM mefenamic acid, the waveform of K41E still showed WT-like delayed current activation and tail current decay (data not shown). Although there was once again no change in the slope and shape of the G-V relationship (data not shown), a significant right shift in the $V_{1/2}$ of activation compared to control was seen with 100 μM mefenamic acid ($\Delta V_{1/2}$ for K41E with 100 μM: +24.9 mV) (Table 2, Fig. 7D). Even in the presence of 1 mM mefenamic acid, there was no effect on the slope and shape of the G-V relationship but still a right shift in $V_{1/2}$ of activation compared to control ($\Delta V_{1/2}$ for K41E with 1 mM: +38.1 mV) (Table 2, Fig. 7D).

In contrast, much like G40C, treatment with 100 μM mefenamic acid transformed the slowly activating waveform of K41R (Fig. 7C upper left panel) into one which has an instantaneous

current and inhibited tail current decay (Fig. 7C lower left panel) characteristic of mefenamic acid's effect on WT EQ $I_{Ks.}$ Mefenamic acid also significantly altered the shape of the K41R G-V relationship (Fig. 7C right panel) when an interpulse interval of 15 s was used. This effect on the shape of the K41R G-V relationship however, was visually less dramatic than that of G40C and WT EQ $I_{Ks}$ (WT EQ $I_{Ks}$ G-V plots in control and 100 μM mefenamic acid both with an interpulse interval of 15 s is overlaid on Fig.7C right panel for comparison; $\Delta V_{1/2}$: -110 mV). Despite this, the effect mefenamic acid had on the G-V relationship of K41R was also dependent on the interpulse interval (data not shown). A shorter interpulse interval of 7 s produced a more dramatically altered G-V relationship and more leftward shift in $V_{1/2}$ than when the interpulse interval was 15 s (data not shown). Additionally, mefenamic acid also resulted in a significant leftward shift in the $V_{1/2}$ of activation of K41R ($\Delta V_{1/2}$: -46.2 mV) (Table 2, Fig. 7D). These results clearly show that residue K41, and especially the charge on this residue is important in facilitating mefenamic acid's modulation of $I_{Ks}$ gating kinetics.

## Discussion

Previous studies have shown that mefenamic acid increases activation of $I_{Ks}$ current and slows tail current decay, but curiously, all of these have only used a single concentration of drug (100 µM). Generally, mefenamic acid effects are restricted to complexes of KCNQ1 and KCNE1 (Busch et al., 1994, 1997; Unsöld et al., 2000), although Abitbol et al. (1999) suggested that mefenamic acid may also facilitate KCNQ1 expressed alone in oocytes. Most studies have not shown that facilitation of $I_{Ks}$ is accompanied by dramatic changes in the current activation time course, except for Unsöld (2000). In this study we confirm that mefenamic acid enhances $I_{Ks}$ activity (Fig. 1C), but not KCNQ1 alone (Fig. 5A), and that this effect is specific to $I_{Ks}$ given that the large instantaneous current was blocked by HMR1556 (Fig. 1D), and no effect on endogenous currents was seen in untransfected cells treated with increasing concentrations of mefenamic acid (Fig. 1B). Following validation of these previous findings we further defined the concentration dependence, effect of interpulse interval, stoichiometry dependence, effect on single channel conductance and the KCNE1 regulatory sites for mefenamic acid actions on $I_{Ks}$.

## Mefenamic acid actions on saturated complexes of $I_{Ks}$ (EQ)

Increasing concentrations of mefenamic acid (1, 10, and 30 µM) have been used to confirm the functional effect of activating $I_{Ks}$ in pre-constricted rat mesenteric arteries ($E_{max}$ of 96.1%) (Chadha et al., 2012), but as noted above, regardless of the expression system, a single concentration of 100 µM has been used to characterize the electrophysiological actions of mefenamic acid on $I_{Ks}$. One striking effect is the induction of instantaneous current and reduction in the overall time-dependent slow activation of $I_{Ks}$ (Fig. 1C). These current changes were used to define the concentration-dependence of mefenamic effects on $I_{Ks}$, giving an $EC_{50}$ and $n^H$ of 60 µM and 0.49, respectively

(Fig. 2). An $n^H$ of <1 does not suggest multiple sites of action or positive cooperative binding of mefenamic acid to the channel complex, which is supported by the similar values of $n^H$ for different stoichiometric ratios of KCNQ1:KCNE1 ($n^H = 0.47$ and 0.66 for EQQ and EQQQQ, respectively). The more commonly reported (in all prior studies) action of mefenamic acid is to slow current deactivation (Busch et al., 1994; Magyar et al., 2006; Toyoda et al., 2006) and our experiments also confirmed the marked slowing of tail currents with time constants increasing across the range of repolarizing potentials (e.g. from 0.52 s to 1.24 s at –90 mV, Fig. 4C).

Mefenamic acid has a hyperpolarizing effect on the $I_{Ks}$ I-V and G-V relationships which, in turn, is reflected by a leftward shift in the $V_{1/2}$ of activation. Quantitatively, this hyperpolarization of the $V_{1/2}$ has previously been inconsistently reported (-15 mV in CHO cells and -26 mV in canine ventricular myocytes) (Unsöld et al., 2000; Magyar et al., 2006). In Figure 3, we demonstrated that this inconsistency may be related to mefenamic acid's striking effect on the G-V relationship that results in part from slowed channel deactivation at shorter pulse intervals. Prior studies often did not state intervals between pulses so this cannot be verified.


With a voltage protocol that lasted 5 s and an interpulse interval of 7 s, there was not enough time to allow for complete $I_{Ks}$ deactivation between voltage clamp pulses in the presence of mefenamic acid. As such, an accumulation of current occurred which partly explains the dramatically altered G-V relationship and instantaneous current at this rate (Fig. 3E). We initially hypothesized that if enough time were given to allow for $I_{Ks}$ deactivation, the G-V relationship in the presence of mefenamic acid would mirror that seen in control (in the absence of mefenamic acid). However, even with an interpulse interval of 30 s in the presence of mefenamic acid, when deactivation should be complete, the G-V relationship still showed a significantly large departure in shape,

slope and $V_{1/2}$, when compared to control. At interpulse intervals of 15, 20 and, especially 30 s, there is a flattening of the voltage dependence of the G-V relationship caused by mefenamic acid that suggests a fundamental modification in the way that $I_{Ks}$ senses and/or responds to changes in the transmembrane potential in the presence of the drug.

The single channel data provide support for the whole cell findings. There was no change in maximum channel conductance (Fig. 6) but openings did group towards higher open subconductance levels (Fig. 6A and 6C) (Werry et al., 2013), which points to enhanced channel activation gating in the presence of mefenamic acid. In addition, data showed a large reduction in the first latency to opening of single channels, with channels opening in mefenamic acid *de novo,* soon after depolarizing pulses were applied. It is important to note that single channel recordings did not indicate that failure of deactivation between pulses was an important factor in the decreased latency to opening (Fig. 6). Thus, single channel kinetics provided significant insight into the changes induced by mefenamic acid seen at the whole cell level. Finally, persistent single channel openings were seen during repolarizations to -40 mV in the presence of mefenamic acid (Fig. 6A), mirroring the slow decay of macroscopic tail currents in the presence of drug (Fig. 4B).

In order to test whether actions of mefenamic acid on activation voltage gating could be sufficient to account for the current changes observed, we used an $I_{Ks}$ model (Zaydman et al., 2014; Westhoff et al., 2019) to simulate drug action, as described in the Methods. Increasing VS forward rates for both activation transitions could account quantitatively for the dose- and rate-dependent action of mefenamic acid (Fig. 8). The effect of increasing drug concentration was to cause the appearance of an instantaneous activating current with a subsequent slower phase, as seen in experimental data

(Figs. 1 and 2). At the highest concentrations, the slow activating phase of current was almost

abolished in simulations (Fig. 8A). The Normalized Response relationship was simulated at a

range of drug concentrations and was fit to a Hill equation with an $EC_{50}$ of 78.6 μM, close that

found experimentally (60 μM), and with a Hill slope of 0.81, compared with 0.49 to 0.66 found

for EQ and EQQQQ, respectively. The action of mefenamic acid was also simulated for step

voltage clamp pulses from -80 mV to +100 mV given every 7 s and 15 s (Figs. 8C-D). The

complete set of simulated currents during the increasing amplitude clamp steps for all four

conditions are shown in Figure 8C, with the blue tracings in control and mefenamic acid in red.

The 7 s interval protocol lasts ~130 s in total and the longer 15 s interval protocol lasts ~285 s. The

effect of mefenamic acid was to increase peak current at both rates, especially at more negative

potentials, as can be clearly seen. The tail currents from these protocols plotted as a function of

voltage (Fig. 8D) give G-V relations, and as seen experimentally (Fig. 3E), the effect of rate was

to cause a minor slope change under control conditions, but a large hyperpolarizing shift was seen

in the presence of mefenamic acid, which was greater at 7 s than at 15 s.


**Mefenamic acid action is diminished with fewer KCNE1 subunits in the $I_{Ks}$ channel complex**

As the KCNQ1:KCNE1 stoichiometry of $I_{Ks}$ is likely variable *in vivo* (Dvir et al., 2014),

understanding the effect of mefenamic acid on different subunit ratios is extremely important, and

the use of fixed stoichiometry constructs in the present experiments allowed a quantitative

comparison of the action of mefenamic acid on different stoichiometries of $I_{Ks}$ (Murray et al.,

2016). The $V_{1/2}$ of activation for KCNQ1 alone was not altered by mefenamic acid, but with the

partially saturated $I_{Ks}$ complexes, EQQ and EQQQQ, the $V_{1/2}$ of activation was significantly

hyperpolarized (Fig. 5). This hyperpolarization was less dramatic than that seen when $I_{Ks}$ was fully

27

saturated (EQ, Fig. 3E). Similarly, in the dose response curves, the responses of EQQ and EQQQQ to mefenamic acid at all concentrations were significantly less than that of EQ, which further supports the idea that the effect of mefenamic acid on $I_{Ks}$ is stoichiometrically graded.

**Mefenamic acid binding to the $I_{Ks}$ complex**

The binding site for DIDS and mefenamic acid on $I_{Ks}$ has previously been suggested to lie between residues 39-43 on KCNE1, with residue E43 specifically identified as critical for the binding of DIDS (Abitbol et al., 1999). Whether this site and/or other residues in the mapped region are critical for the binding of mefenamic acid to KCNE1, and/or $I_{Ks}$, was not studied. Through mutational analysis, we now show that although mutation of residues E43 and L42 in KCNE1 results in a reduced response to mefenamic acid, residue K41 is critical for the action of mefenamic acid (Fig. 7).

Most of the mutations themselves do have variable effects on the gating of $I_{Ks}$ in the absence of mefenamic acid (Table 2), but importantly K41C has little effect on the position or slope of the $I_{Ks}$ G-V relationship compared to WT EQ. This suggests that K41C does not itself destabilize the normal interactions between KCNQ1 and KCNE1 in the $I_{Ks}$ channel complex, or its ability to respond to applied changes in potential. These results are particularly interesting, taken in the context of the known importance of interactions between KCNQ1 and this region of KCNE to the pathophysiology of short QT syndrome, in which extremely slow deactivation is a feature (Dvir et al., 2014).

The E43C, L42C, and K41E mutations shift the $V_{1/2}$ of $I_{Ks}$ to approximately +70 mV (Table 2), which is opposite to the direction expected if they were inhibiting the interactions between KCNQ1 and KCNE1 (Murray et al., 2016), but which may explain their lesser response to mefenamic acid

(Fig. 7D). The G40C mutant responds almost like WT to mefenamic acid (Supplemental Fig. 1) and, so defines a proximal limit of the critical region. Taken together, the data indicate the primary importance of K41 in the binding of mefenamic acid to the $I_{Ks}$ channel complex, and the response of K41R but not K41E to mefenamic acid suggests the importance of electrostatic rather than steric interactions in this effect.

**Relevance of mefenamic acid activation of $I_{Ks}$ channel currents**

Unlike most other activators that have little effect on $I_{Ks}$ channels with increasingly saturated stoichiometries (Magyar et al., 2006; Gao et al., 2008; Yu et al., 2013), we have shown that mefenamic acid can enhance all $I_{Ks}$ channel complexes of different stoichiometries, suggesting that this molecule or others like it may represent a therapeutic approach to treating LQTS types 1 and 5. Although this is well beyond the scope of the present study, we note that mefenamic acid is presently prescribed at a recommended dosage of 500 mg per day which has been reported to equate to a mean plasma concentration of 82.9 µM (Cryer and Feldman, 1998). This provides little clue towards the amount needed therapeutically to treat LQTS, but such concentrations cause a potent activating effect of mefenamic acid that is also dependent on the stimulus rate, which is important as $I_{Ks}$ primarily contributes to cardiac repolarization at high heart rates. The definitive stoichiometry of $I_{Ks}$ in humans as well as the degree of $I_{Ks}$ channel activation required for a therapeutically beneficial shortening of the QT interval are presently unknown, so we cannot know whether compounds like mefenamic acid could have a beneficial effect in LQTS. We do, however, know that due to the known adverse gastrointestinal effects of COX1 inhibition, and block of other channels such as TRPC, TRPM and TREK channels (Takahira et al., 2005; Klose et al., 2011; Jiang et al., 2012), mefenamic acid itself is unlikely to be a suitable candidate.

**Conclusion**

The KCNQ1 channel alone is insensitive to up to 1 mM mefenamic acid, and the drug increases $I_{Ks}$ channel complex currents dependent upon the number of KCNE1 subunits present, unlike most other activators that have little effect on $I_{Ks}$ channels with increasingly saturated stoichiometries. Single channel studies reveal no change in the maximum conductance, so the instantaneous currents in the presence of mefenamic acid and the prolonged deactivation of tail currents are caused by a voltage-dependent shift of channel gating kinetics towards more negative potentials, and a marked decrease in the voltage sensitivity of the channel. A shift to occupancy of higher subconductance states may also be in part responsible for the increase in peak currents. In-silico modeling of the action of mefenamic acid showed that modulation of VS forward rates could account quantitatively for the drug effects. The ability of mefenamic acid to mediate these gating changes relies on binding to $I_{Ks}$ regulated through K41 on KCNE1 and potentially other residues surrounding it. The presence of mefenamic acid bound to the $I_{Ks}$ channel complex fundamentally alters the ability of the KCNQ1/KCNE1 gating machinery to respond to the transmembrane potential gradient.

## Acknowledgements

## Authorship Contributions

*Participated in research design:* Fedida, Wang, Eldstrom

*Conducted experiments:* Wang, Eldstrom

*Performed data analysis:* Wang, Eldstrom, Fedida

*Wrote or contributed to the writing of the manuscript:* Wang, Fedida, Eldstrom

## References

Abbott GW (2014) Biology of the KCNQ1 Potassium Channel. *New Journal of Science*.1-26.

Abitbol I, Peretz A, Lerche C, Busch AE, and Attali B (1999) Stilbenes and fenamates rescue the

   loss of I KS  channel function induced by an LQT5 mutation and other IsK mutants.

   *EMBO Journal*. **18**:4137-4148.

Bendahhou S, Marionneau C, Haurogne K, Larroque MM, Derand R, Szuts V, Escande D,

   Demolombe S, and Barhanin J (2005) In vitro molecular interactions and distribution of

   KCNE family with KCNQ1 in the human heart. *Cardiovascular Research*. **67**:529-538.

Busch AE, Busch GL, Ford E, Suessbrich H, Lang HJ, Greger R, Kunzelmann K, Attali B, and

   StÅhmer W (1997) The role of the  I  sK  protein in the specific pharmacological

   properties of the  I  Ks  channel complex. *British Journal of Pharmacology*. **122**:187-189.

Busch AE, Herzer T, Wagner CA, Schmidt F, Raber G, Waldegger S, and Lang F (1994)

   Positive regulation by chloride channel blockers of I sK  channels expressed in  Xenopus

   oocytes. *Mol.Pharmacol.* **46**:750-753.

Chadha PS, Zunke F, Davis AJ, Jepps TA, Linders JT, Schwake M, Towart R, and Greenwood

   IA (2012) Pharmacological dissection of K(v)7.1 channels in systemic and pulmonary

   arteries. *Br J Pharmacol*. **166**:1377-1387.

Colquhoun D, and Hawkes AG. 1995. A Q-matrix cookbook: how to write only one program to

   calculate the single-channel and macroscopic predictions for any kinetic mechanism. *In*

   Single-Channel Recording. B. Sakmann and E. Neher, editors. Springer. 589-633.

Cryer B, and Feldman M (1998) Cyclooxygenase-1 and cyclooxygenase-2 selectivity of widely

   used nonsteroidal anti-inflammatory drugs. *Am J Med*. **104**:413-421.

Doolan GK, Panchal RG, Fonnes EL, Clarke AL, Williams DA, and Petrou S (2002) Fatty acid augmentation of the cardiac slowly activating delayed rectifier current (I Ks ) is conferred by  hminK *FASEB Journal*. **16**:NIL57-NIL71.

Dvir M, Peretz A, Haitin Y, and Attali B (2014) Recent molecular insights from mutated IKS channels in cardiac arrhythmia. *Curr Opin Pharmacol*. **15**:74-82.

Eldstrom J, and Fedida D (2011) The voltage-gated channel accessory protein KCNE2: multiple ion channel partners, multiple ways to long QT syndrome. *Expert.Rev.Mol.Med.* **13**:e38.

Eldstrom J, Wang Z, Werry D, Wong N, and Fedida D (2015) Microscopic mechanisms for long QT syndrome type 1 revealed by single-channel analysis of I(Ks) with S3 domain mutations in KCNQ1. *Heart Rhythm.* **12**:386-394.

Gao Z, Xiong Q, Sun H, and Li M (2008) Desensitization of chemical activation by auxiliary subunits: convergence of molecular determinants critical for augmenting KCNQ1 potassium channels. *J Biol Chem*. **283**:22649-22658.

Gögelein H, Brüggemann A, Gerlach U, Brendel J, and Busch AE (2000) Inhibition of  I  Ks channels by HMR 1556. *Naunyn-Schmiedebergs Archives of Pharmacology*. **362**:480-488.

Hedley PL, Jorgensen P, Schlamowitz S, Wangari R, Moolman-Smook J, Brink PA, Kanters JK, Corfield VA, and Christiansen M (2009) The Genetic Basis of Long QT and Short QT Syndromes: A Mutation Update. *Human Mutation*. **30**:1486-1511.

Jiang H, Zeng B, Chen GL, Bot D, Eastmond S, Elsenussi SE, Atkin SL, Boa AN, and Xu SZ (2012) Effect of non-steroidal anti-inflammatory drugs and new fenamate analogues on TRPC4 and TRPC5 channels. *Biochem Pharmacol*. **83**:923-931.

Klose C, Straub I, Riehle M, Ranta F, Krautwurst D, Ullrich S, Meyerhof W, and Harteneck C

(2011) Fenamates as TRP channel blockers: mefenamic acid selectively blocks TRPM3.

*Br J Pharmacol*. **162**:1757-1769.

Liin SI, Barro-Soria R, and Larsson HP (2015) The KCNQ1 channel - remarkable flexibility in

gating allows for functional versatility. *J.Physiol*. **593**:2605-2615.

Lundquist AL, Manderfield LJ, Vanoye CG, Rogers CS, Donahue BS, Chang PA, Drinkwater

DC, Murray KT, and George AL, Jr. (2005) Expression of multiple KCNE genes in

human heart may enable variable modulation of I(Ks). *J.Mol.Cell Cardiol.* **38**:277-287.

Magyar J, Horvath B, Banyasz T, Szentandrassy N, Birinyi P, Varro A, Szakonyi Z, Fulop F, and

Nanasi PP (2006) L-364,373 fails to activate the slow delayed rectifier K+ current in

canine ventricular cardiomyocytes. *Naunyn Schmiedebergs Arch Pharmacol*. **373**:85-89.

Manderfield LJ, and George AL, Jr. (2008) KCNE4 can co-associate with the I(Ks) (KCNQ1-

KCNE1) channel complex. *FEBS J.* **275**:1336-1349.

Morin TJ, and Kobertz WR (2008) Counting membrane-embedded KCNE beta-subunits in

functioning K+ channel complexes. *Proc.Natl.Acad.Sci.U.S.A*. **105**:1478-1482.

Mruk K, and Kobertz WR (2009) Discovery of a novel activator of KCNQ1-KCNE1 K channel

complexes. *PLoS One*. **4**:e4236.

Murray CI, Westhoff M, Eldstrom J, Thompson E, Emes R, and Fedida D (2016) Unnatural

amino acid photo-crosslinking of the channel complex demonstrates a KCNE1:KCNQ1

stoichiometry of up to 4:4. *Elife.* **5**.

Nakajo K, Ulbrich MH, Kubo Y, and Isacoff EY (2010) Stoichiometry of the KCNQ1-KCNE1

ion channel complex. *Proc.Natl.Acad.Sci.U.S.A*. **107**:18862-18867.

Plant LD, Xiong D, Dai H, and Goldstein SA (2014) Individual IKs channels at the surface of mammalian cells contain two KCNE1 accessory subunits. *Proc.Natl.Acad.Sci.U.S.A*. **111**:E1438-E1446.

Sanguinetti MC, Curran ME, Zou A, Shen J, Spector PS, Atkinson DL, and Keating MT (1996) Coassembly of K v LQT1 and minK (IsK) proteins to form cardiac I Ks potassium channel. *Nature*. **384**:80-83.

Santiago-Castillo JA, Covarrubias M, Sánchez-Rodríguez JE, Perez-Cornejo P, and Arreola J (2010) Simulating complex ion channel kinetics with IonChannelLab. *Channels (Austin)*. **4**:422-428.

Splawski I, Shen J, Timothy KW, Lehmann MH, Priori S, Robinson JL, Moss AJ, Schwartz PJ, Towbin JA, Vincent GM, and Keating MT (2000) Spectrum of mutations in long-QT syndrome genes. KVLQT1, HERG, SCN5A, KCNE1, and KCNE2. *Circulation*. **102**:1178-1185.

Takahira M, Sakurai M, Sakurada N, and Sugiyama K (2005) Fenamates and diltiazem modulate lipid-sensitive mechano-gated 2P domain K(+) channels. *Pflugers Arch*. **451**:474-478.

Thompson E, Eldstrom J, Westhoff M, McAfee D, Balse E, and Fedida D (2017) cAMP-dependent regulation of IKs single-channel kinetics. *J Gen Physiol*. **149**:781-798.

Toyoda F, Ueyama H, Ding WG, and Matsuura H (2006) Modulation of functional properties of KCNQ1 channel by association of KCNE1 and KCNE2. *Biochemical and Biophysical Research Communications*. **344**:814-820.

U.S. FDA (2008) Food and Drug Administration; PONSTEL® (Mefenamic Acid Capsules, USP). [Internet]. Available from: .

*https://www.accessdata.fda.gov/drugsatfda_docs/label/2008/015034s040lbl.pdf*.

Unsöld B, Kerst G, Brousos H, HÅbner M, Schreiber R, Nitschke R, Greger R, and Bleich M

(2000) KCNE1 reverses the response of the human K + channel KCNQ1 to cytosolic pH

changes and alters its pharmacology and sensitivity to temperature. *Pflugers Archiv*

*European Journal of Physiology*. **441**:368-378.

Werry D, Eldstrom J, Wang Z, and Fedida D (2013) Single-channel basis for the slow activation

of the repolarizing cardiac potassium current, I(Ks). *Proc.Natl.Acad.Sci.U.S.A*.

**110**:E996-1005.

Westhoff M, Eldstrom J, Murray CI, Thompson E, and Fedida D (2019) I Ks ion-channel pore

conductance can result from individual voltage sensor movements. *Proc Natl Acad Sci U*

*S A*. **116**:7879-7888.

Westhoff M, Murray CI, Eldstrom J, and Fedida D (2017) Photo-Cross-Linking of IKs

Demonstrates State-Dependent Interactions between KCNE1 and KCNQ1. *Biophys J*.

**113**:415-425.

Yu H, Lin Z, Mattmann ME, Zou B, Terrenoire C, Zhang H, Wu M, McManus OB, Kass RS,

Lindsley CW, Hopkins CR, and Li M (2013) Dynamic subunit stoichiometry confers a

progressive continuum of pharmacological sensitivity by KCNQ potassium channels.

*Proc.Natl.Acad.Sci.U.S.A*. **110**:8732-8737.

Zaydman MA, Kasimova MA, McFarland K, Beller Z, Hou P, Kinser HE, Liang H, Zhang G,

Shi J, Tarek M, and Cui J (2014) Domain-domain interactions determine the gating,

permeation, pharmacology, and subunit modulation of the IKs ion channel. *Elife*.

**3**:e03606.

Zheng Y, Zhu X, Zhou P, Lan X, Xu H, Li M, and Gao Z (2012) Hexachlorophene is a potent

KCNQ1/KCNE1 potassium channel activator which rescues LQTs mutants. *PLoS One*.

**7**:e51820.

**Footnotes**

**Figure Legends**

**Figure 1. Mefenamic acid increases EQ current expressed in mammalian cells.** (A) Molecular

structure of mefenamic acid. Nitrogen and oxygen atoms are depicted in blue and red, respectively.

(B) Response of an untransfected cell to mefenamic acid (abbreviated as 'Mef' in this and all other

figures). Left panel shows representative current traces in the absence of mefenamic acid (control;

black) and after the addition of 10 µM - 1 mM mefenamic acid as indicated (grey). Right panel

shows $I_{max} - I_{min}$ (peak to steady-state difference currents) vs. sweep number during the addition

of different concentrations of mefenamic acid (solid grey lines). (C) Dose response of EQ currents

to mefenamic acid. Left panel shows currents in control (black) and in response (grey) to different

concentrations of mefenamic acid. Right panel shows the data in a diary plot. (D) Response of EQ

to 1 µM HMR1556 in the presence of mefenamic acid (100 µM mefenamic acid preincubation for

approximately 30 min, data not shown). Complete block by HMR1556 is indicated by the red

arrows. Left panel shows 100 µM mefenamic acid alone (black), and in response to 1 µM

HMR1556 (grey). Right panel shows the data in an initial peak amplitude vs sweep number diary

plot. The solid grey line indicates addition of HMR1556. All currents (Figs. 1B-D) were obtained

by pulsing to +60 mV for 4 s followed by a pulse to -40 mV for 0.9 s. The interpulse interval was

15 s. Holding potential was -80 mV. Dotted baselines denote the zero current level.

**Figure 2. Mefenamic acid dose-response curves for EQ.** All currents used to calculate dose-

response curves were obtained using the same protocol described in Fig. 1. (A) Representative

dose-response calculation and curve. Upper panel shows representative $I_{max} - I_{min}$ (peak to steady-

state difference current) measurements in the absence of mefenamic acid (black) and in the

presence of 300 µM mefenamic acid (grey). Lower panel shows $I_{max} - I_{min}$ vs log concentration of mefenamic acid, data from Fig. 1C. (B) Mean log concentration-response curve for EQ (n = 3-5 at each concentration); $EC_{50}$ = 60 [38, 89; 95% CI] µM; $n^H$ = 0.49 [0.39, 0.60; 95% CI]). Responses were normalized to the maximum peak to steady-state difference current in the absence of mefenamic acid and subtracted from 1.0 (see Methods).

**Figure 3. Mefenamic acid rate-dependently hyperpolarizes EQ I-V and G-V relationships.**
Currents were obtained using a 4 s step protocol with pulses from -150 mV to +100 mV, followed by a repolarizing step to -40 mV for 1 s. (A) Currents are shown for EQ in the absence (control; interpulse interval was 15 s; upper panel), and the presence of 100 µM mefenamic acid (interpulse interval was 30 s; lower panel). (B) I-V plots of current at the end of the 4 s depolarizing pulses in control (black triangles), and mefenamic acid (grey triangles), data from Fig. 3A. (C) G-V relationships obtained from peak initial tail currents in control ($V_{1/2}$ = 24.0 mV; $k$ = 24.0 mV; black circles) and mefenamic acid ($V_{1/2}$ = -2.4 mV; $k$ = 65.4 mV; grey circles), data from Fig. 3A. (D) and (E) Effect of different interpulse intervals on I-V (triangles) and G-V (circles) plots in control and mefenamic acid. Intervals were 7 s (n=1; orange), and 15 s (n=4; black) in control; and, 7 s (red), 15 s (green), 20 s (blue) or 30 s (purple) in mefenamic acid (n=4-6). For G-V plots, Boltzmann fits were, for 7 s ($V_{1/2}$ =17.8 mV; $k$ = 12.9 mV) and 15s ($V_{1/2}$ = 23.9 mV; $k$ = 20.4 mV) in control; and, for 7 s ($V_{1/2}$ = -108 mV; $k$ = 6.9 mV), 15 s ($V_{1/2}$ = -86.5 mV; $k$ = 23.2 mV), 20 s ($V_{1/2}$ = -80.5 mV; $k$ = 53.3 mV), and 30 s intervals ($V_{1/2}$ = -13.1 mV; $k$ = 57.2 mV) in mefenamic acid (see Table 1). $V_{1/2}$ values for mefenamic acid compared with control were significantly different at all intervals (Table 1).

**Figure 4. Mefenamic acid slows EQ deactivation.** Tail currents were obtained by pulsing to +60 mV for 4 s to activate $I_{Ks}$ current, followed by a 4 s pulse to a range of potentials from -40 mV to -150 mV in 10 mV steps. Holding potential was -90 mV. (A) Representative tail currents (black) fit with a single exponential curve (blue lines) for EQ $I_{Ks}$ in the absence of mefenamic acid. (B) Representative tail currents (black) fit with a single exponential curve (blue lines) for EQ $I_{Ks}$ in the presence of 100 µM mefenamic acid. (C) Time constants of deactivation ($\tau_{deact}$) vs different membrane potentials for EQ $I_{Ks}$ in the absence (n=3, black circles) and in the presence of 100 µM mefenamic acid (n= 5, grey circles). \*\*, \*\*\* and \*\*\*\* denotes significance where p = 0.0089, p = 0.0003 and p < 0.0001, respectively.

**Figure 5. Effect of $I_{Ks}$ stoichiometry on response to 100 µM mefenamic acid.** The currents and conductance-voltage plots (Figs. 5A-C) were obtained using the protocols described in Fig. 3 with a 15 s interpulse interval. For each stoichiometry (see Methods), representative currents are shown in the absence of (control; upper left panel) and in the presence of 100 µM mefenamic acid (lower left panel). Right panels show the corresponding G-V plots in control (black circles) and presence of mefenamic acid (grey circles). Boltzmann fits were: (A) for Q1 in control (n = 5): $V_{1/2}$ = -20.5 mV, $k$ = 8.8 mV; and, in mefenamic acid (n = 4): $V_{1/2}$ = -25.6 mV, $k$ = 14.9 mV; (B) for EQQQQ $I_{Ks}$ in control (n = 4): $V_{1/2}$ = -1.5 mV, $k$ = 18.1 mV; and, in mefenamic acid (n = 4): $V_{1/2}$ = -20.8 mV, $k$ = 18.3 mV; (C) for EQQ $I_{Ks}$ in control (n = 5): $V_{1/2}$ = 15.4 mV, $k$ = 20.6 mV; and in mefenamic acid (n = 4) $V_{1/2}$ = -1.6 mV, $k$ = 20.3 mV (See Table 2). (D) Normalized log concentration-response relationships for EQ, EQQ and EQQQQ $I_{Ks}$ were obtained using the analysis method described in Fig. 2. For EQ $I_{Ks}$: $EC_{50}$ = 60 [38, 89; 95% CI] µM, $n^H$ = 0.49 [0.39, 0.60; 95% CI], green diamonds, data from Fig. 2B; for EQQ $I_{Ks}$: $EC_{50}$ = 615 [422, 955; 95% CI]

μM, $n^H$ = 0.47 [0.37, 0.60; 95% CI], blue diamonds; and for EQQQQ $I_{Ks}$: EC$_{50}$ = 902 [663, 1383; 95% CI] μM, $n^H$ = 0.66 [0.49, 0.87; 95% CI], red diamonds. For each construct, n = 3-5 at each concentration. **, *** and **** denotes a significantly different response when compared to EQ $I_{Ks}$ and, where p<0.05, p<0.0005 and p<0.0001, respectively.

**Figure 6. Mefenamic acid increases the open probability of $I_{Ks}$ and not the conductance.** (A) Single channel currents were obtained using the protocol shown. The sweep to sweep interval was 10 s. Representative single channel traces are shown for control EQ (top 3 sweeps) and from the same cell after approximately 23 min of 100 μM mefenamic acid exposure (bottom 3 sweeps). Black dotted lines indicate the 0.5 pA level. Blue lines indicate the zero current level. (B) Ensemble averages of 18 active sweeps each of EQ (blue) and in the presence of 100 μM mefenamic acid (red).  (C) All-points histograms of the 3 control EQ sweeps (blue) and the 3 sweeps in presence of mefenamic acid (red) shown in Fig. 6A.

**Figure 7. Mapping the mefenamic acid regulatory sites on KCNE1.** The currents and conductance-voltage (G-V) plots (Figs. 7A-C) were obtained using the protocols described in Fig 3. The interpulse interval was 15 s. For each EQ $I_{Ks}$ mutant, representative currents are shown in the absence of (control; upper left panel) and in the presence of 100 μM mefenamic acid (lower left panel). Right panels show the corresponding G-V plots in control, (black circles) and presence of 100 μM (grey circles) and 1 mM (purple circles) mefenamic acid. WT EQ $I_{Ks}$ in control (blue triangles) and presence of 100 μM mefenamic acid (red triangles), both with a 15 s interpulse interval is overlaid in Fig 7C (data from Fig 3E). Boltzmann fits were: (A) for L42C in control (n = 3): V$_{1/2}$ =  68.9 mV, $k$ = 21.5 mV; and, in 100 μM mefenamic acid (n = 3): V$_{1/2}$ = 31.8  mV, $k$ =

14.8 mV; (B) for K41C in control (n = 6): $V_{1/2}$ = 17.1 mV, $k$ = 19.7 mV; and, in 100 µM mefenamic

acid (n = 4): $V_{1/2}$ = 11.3 mV, $k$ = 19.3 mV; and, in 1 mM mefenamic acid (n = 4): $V_{1/2}$ = 14.0 mV,

$k$ = 18.3 mV; (C) for K41R in control (n = 3): $V_{1/2}$ = 72.7 mV, $k$ = 20.8 mV; and in 100 µM

mefenamic acid (n = 4) $V_{1/2}$ = 26.6 mV, $k$ = 49.3 mV (Table 2). (D) Change in $V_{1/2}$ ($\Delta V_{1/2}$) for

each EQ $I_{Ks}$ mutant in control *vs*. mefenamic acid (n = 3-6 at each concentration). *, **, *** and

**** denotes a significant change in $V_{1/2}$ comparing control to the presence of mefenamic acid,

where p < 0.03, p = 0.0011, p = 0.0003 and p<0.0001, respectively.

**Figure 8. Modeling the effect of mefenamic acid on VS activation.** (A) The effect of 100 µM

(red) and 1 mM (pink) mefenamic acid on EQ $I_{Ks}$ currents, compared with control (blue) as

reproduced by the model. Voltage pulse was from a holding potential of -90 mV to +60 mV for 4

s, followed by repolarization to -50 mV for 2 s. Pulses were given every 15 s. Mefenamic acid is

assumed to affect the VS forward rates for both resting to intermediate and intermediate to

activated transitions in a concentration-dependent manner, see Methods for details and model

parameters. Data in (B) show model response to 10, 30, 100, 300 µM and 1 mM mefenamic acid,

simulating data from Figures 1C and 2B. Line fit using Hill equation with $EC_{50}$ = 78.6 µM, $n^H$ =

0.81. (C) Effect of pulse rate on current-voltage relationships in control (blue) and 100 µM

mefenamic acid (red). Continuous simulated current records are shown. Pulse protocol was from

a holding potential of -90 mV to steps between -80 and +100 mV in 10 mV, applied every 7s or

every 15 s. Total protocol duration was thus 133 s or 285 s, respectively. (D) G-V relationships

from tail currents in (C). Boltzmann fits were: 7 s ($V_{1/2}$ = 14.2 mV; $k$ = 17.0 mV) and 15 s ($V_{1/2}$ =

27.1 mV; $k$ = 17.7 mV) in control; and, 7 s ($V_{1/2}$ = -77.3 mV; $k$ = 25.2 mV) and 15 s ($V_{1/2}$ = -50.8

mV; $k$ = 26.1 mV) in mefenamic acid. The ordinate label 'a.u.' = arbitrary units.

**Table 1.** $V_{1/2}$ of activation (mV) and slope value ($k$-factor, mV) in the absence and presence of

100 μM mefenamic acid for EQ $I_{Ks}$ at different interpulse intervals. ± denotes standard deviation

with the p-value indicating statistical difference in $V_{1/2}$ compared to control as determined using

a One-way Anova and Bonferroni multiple comparisons test.

| | $V_{1/2}$ | $k$-factor | $n$ | |
|---|---|---|---|---|
| **EQ Control: Interpulse Interval 15 s** | 23.9 ± 3.7 | 20.4 ± 2.9 | 4 | **p-value** |
| **EQ + Mefenamic Acid: Interpulse Interval 7 s** | -108 ± 9.0 | 6.9 ± 7.7 | 6 | <0.0001 |
| **EQ + Mefenamic Acid Interpulse Interval 15 s** | -86.5 ± 14.8 | 23.2 ± 11.2 | 4 | <0.0001 |
| **EQ + Mefenamic Acid Interpulse Interval 20 s** | -80.5 ± 18.2 | 53.3 ± 15.3 | 5 | <0.0001 |
| **EQ + Mefenamic Acid Interpulse Interval 30 s** | -13.1 ± 14.9 | 57.2 ± 15.4 | 6 | 0.0057 |

**Table 2.** $V_{1/2}$ of activation (mV) and slope value (*k*-factor, mV) in the absence and presence of mefenamic acid for mutant EQ $I_{Ks}$ and different stoichiometrically saturated WT $I_{Ks}$. ± denotes standard deviation with the p-value indicating statistical difference in $V_{1/2}$ compared to control as determined using a One-way Anova and Bonferroni multiple comparisons test.

| | Control | | | 100 µM or 1 mM Mefenamic Acid * | | | $\Delta V_{1/2}$ | p-value |
|---|---|---|---|---|---|---|---|---|
| | *$V_{1/2}$* | *K-factor* | *n* | *$V_{1/2}$* | *k-factor* | *n* | | |
| **EQ** | 23.9 ± 3.7 | 20.4 ± 2.9 | 4 | -86.5 ± 14.8 | 23.2 ± 11.2 | 4 | -110 | <0.0001 |
| **EQQ** | 15.4 ± 2.6 | 20.6 ± 3.9 | 5 | -1.6 ± 2.7 | 20.3 ± 4.5 | 4 | -17.1 | 0.0472 |
| **EQQQQ** | -1.5 ± 5.0 | 18.1 ± 1.1 | 4 | -20.8 ± 3.7 | 18.3 ± 3.0 | 4 | -19.3 | 0.0298 |
| **Q1** | -20.5 ± 1.4 | 8.8 ± 2.9 | 5 | -25.6 ± 12.9 | 14.9 ± 4.7 | 4 | -5.1 | NS |
| **E43C** | 70.8 ± 3.5 | 27.0 ± 5.5 | 4 | 46.4 ± 8.4 | 29.1 ± 3.4 | 4 | -24.4 | 0.0228 |
| **L42C** | 68.9 ± 2.6 | 21.5 ± 6.4 | 3 | 31.8 ± 0.6 | 14.8 ± 7.4 | 3 | -37.2 | 0.0011 |
| **K41C** | 17.1 ± 4.6 | 19.7 ± 4.7 | 6 | 11.3 ± 1.6 | 19.3 ± 1.7 | 4 | -5.8 | NS |
| | | | | 14.0 ± 6.2 | 18.3 ± 3.6 | 4 | -3.2 | NS |
| **K41E** | 76.5 ± 5.5 | 24.2 ± 0.8 | 4 | 102 ± 7.5 | 25.0 ± 2.0 | 4 | 24.9 | 0.0189 |
| | | | | 115 ± 8.0 | 25.6 ± 1.7 | 3 | 38.1 | 0.0003 |
| **K41R** | 72.7 ± 5.8 | 20.8 ± 3.2 | 3 | 26.6 ± 21.1 | 49.3 ± 19.4 | 4 | -46.2 | <0.0001 |
| **G40C** | 38.2 ± 11.8 | 20.0 ± 2.2 | 4 | -37.9 ± 23.5 | ~40.3 | 3 | -76.1 | <0.0001 |

NS, not significant. * Mefenamic acid dose was either 100 µM (where applicable upper row values) or 1 mM (where applicable lower row values). Given the dramatic effect mefenamic acid has on the G-V relationship for some constructs, Boltzmann curves could not be properly fit in some cases.
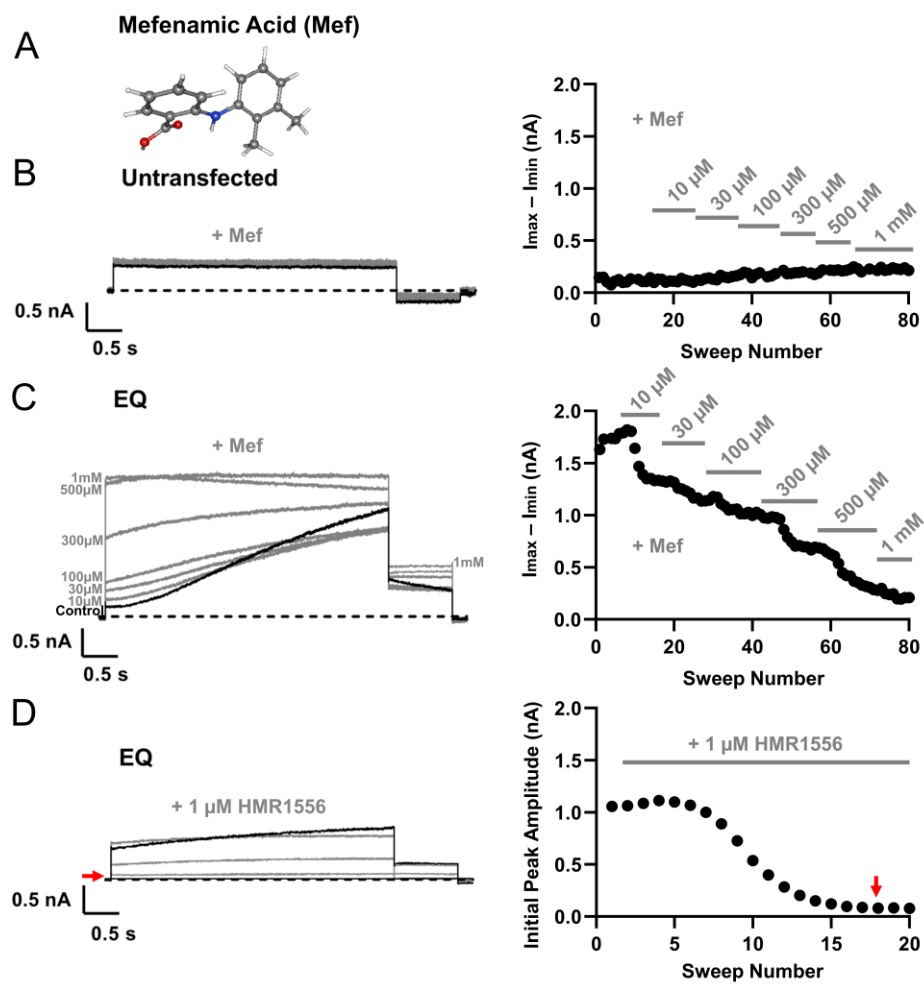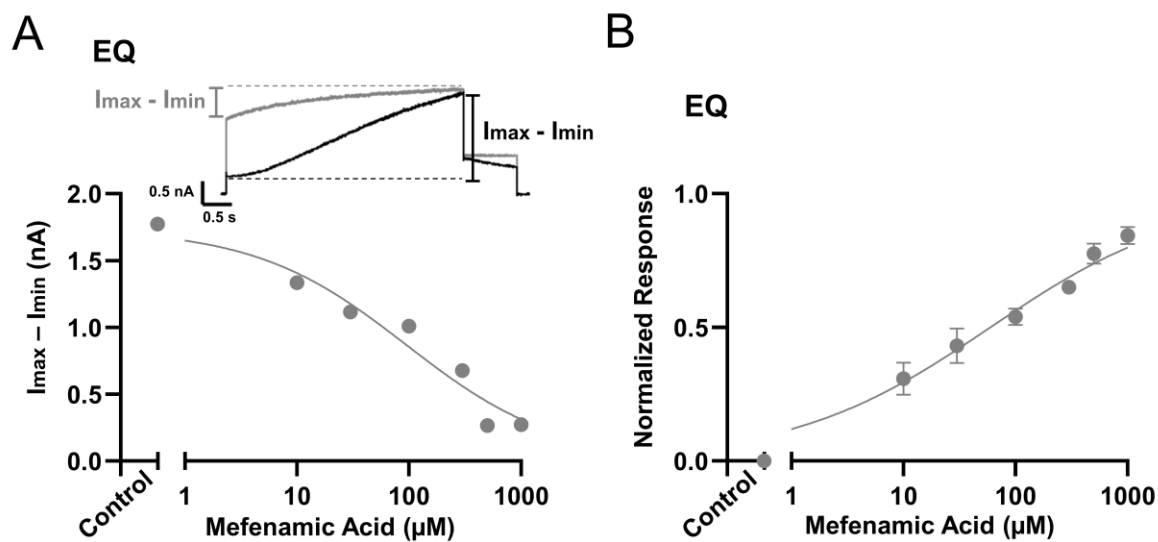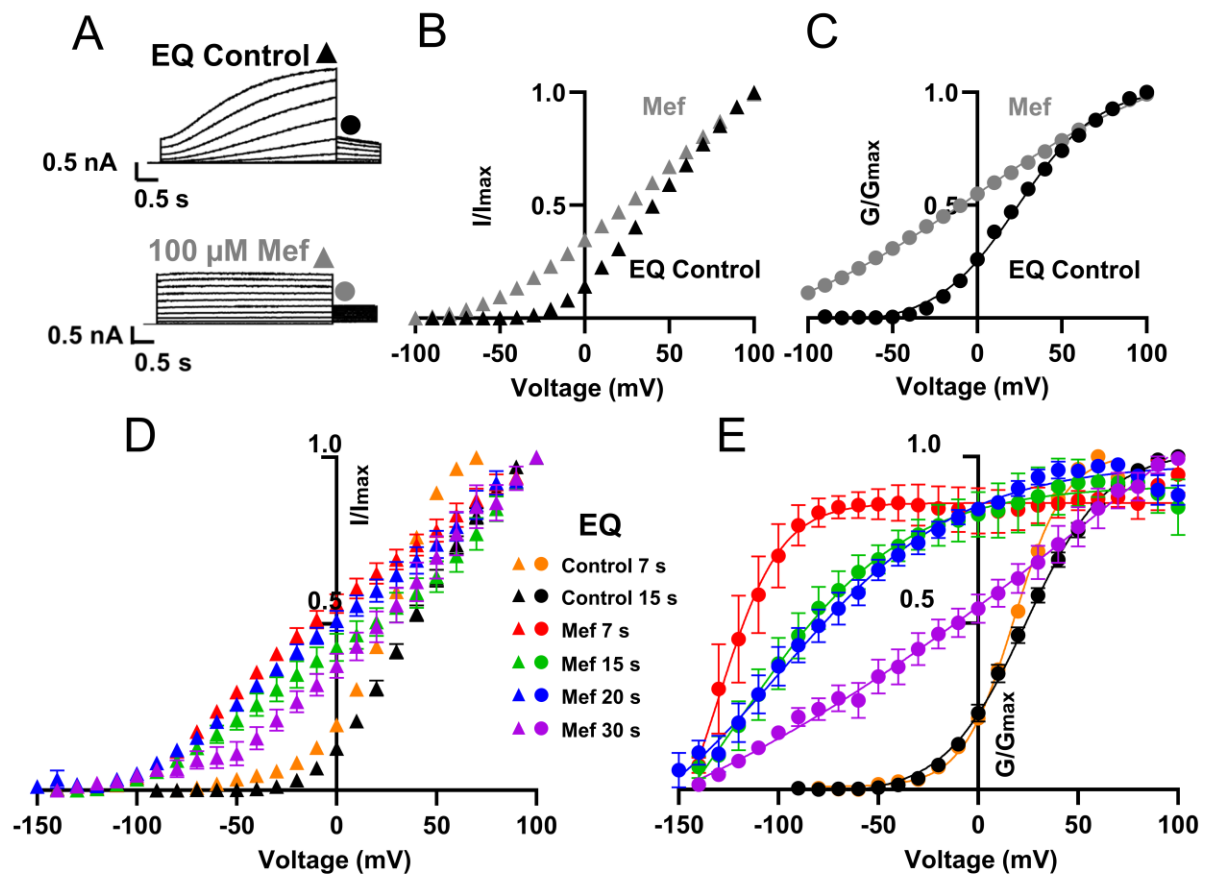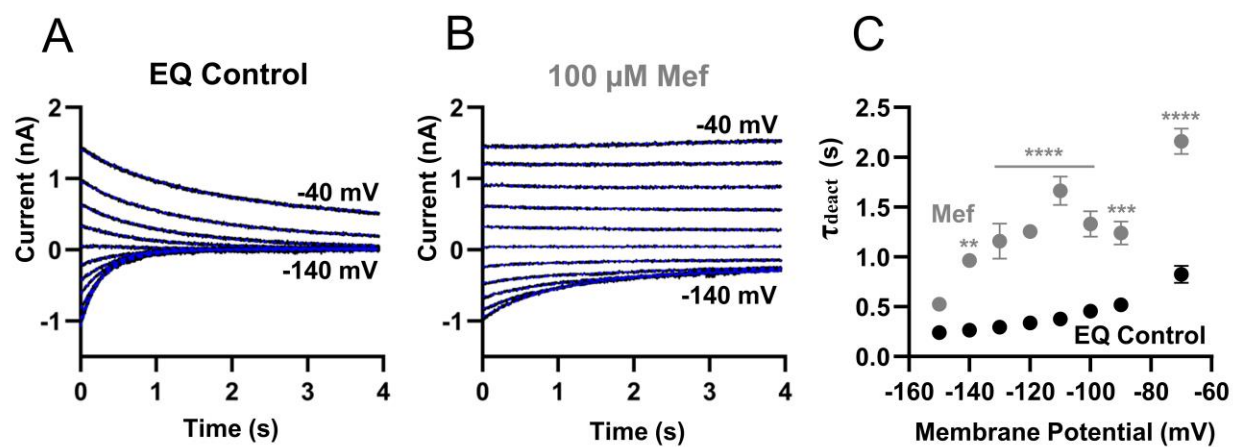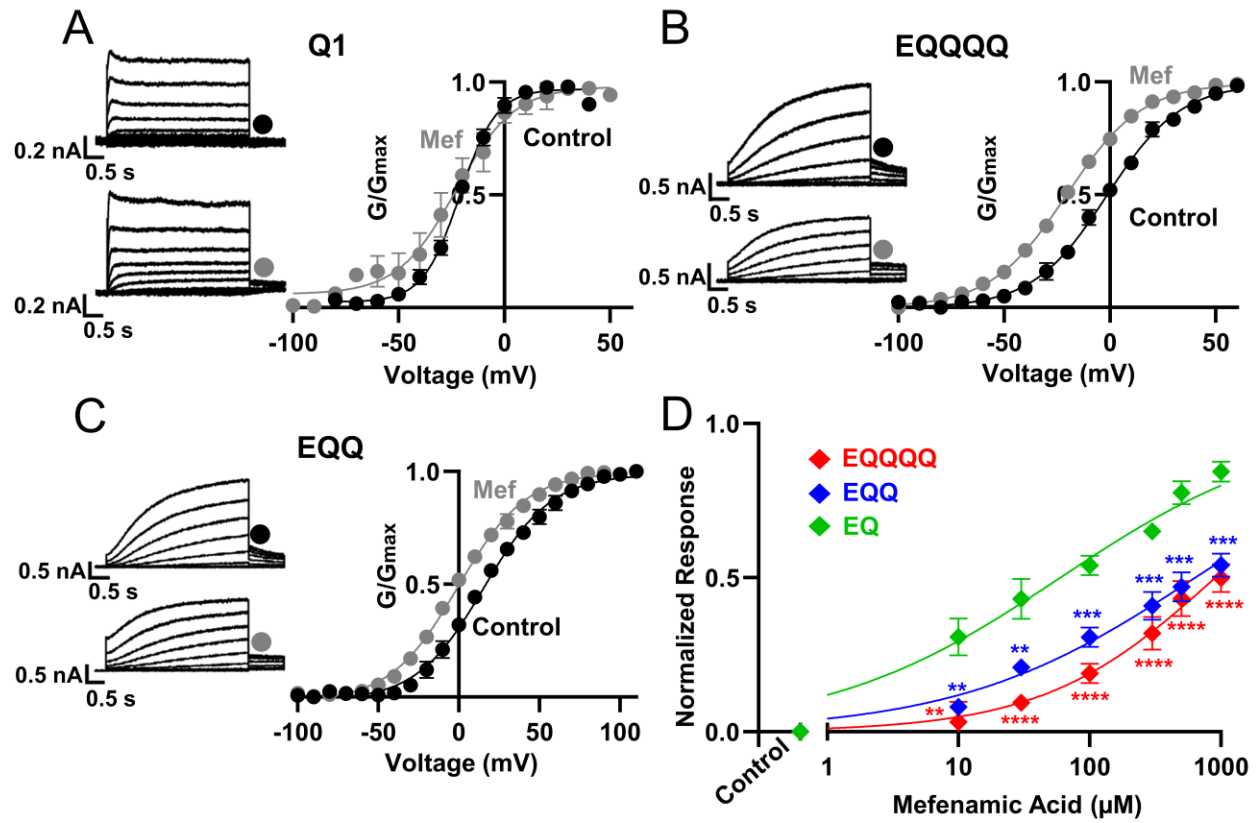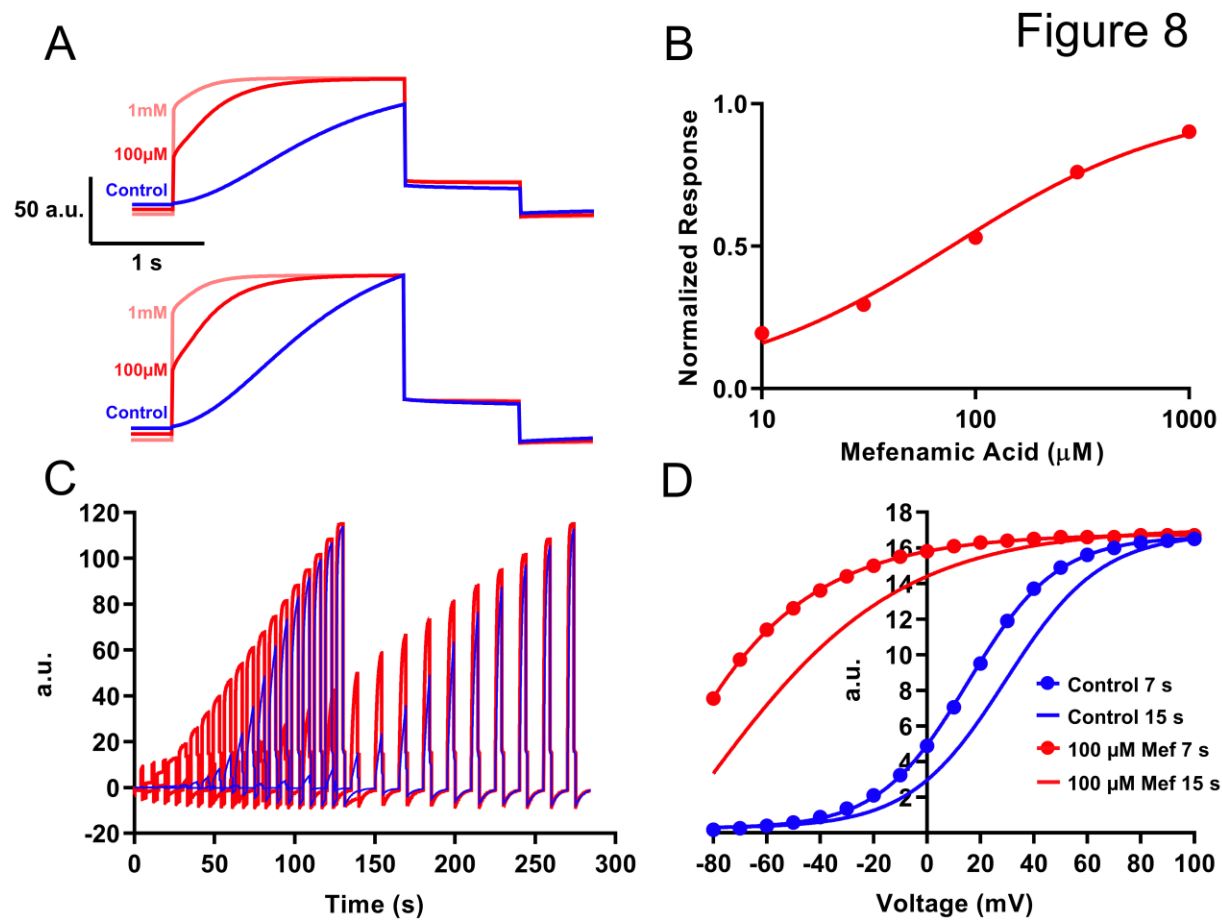
Figure 1

Figure 2

Figure 3
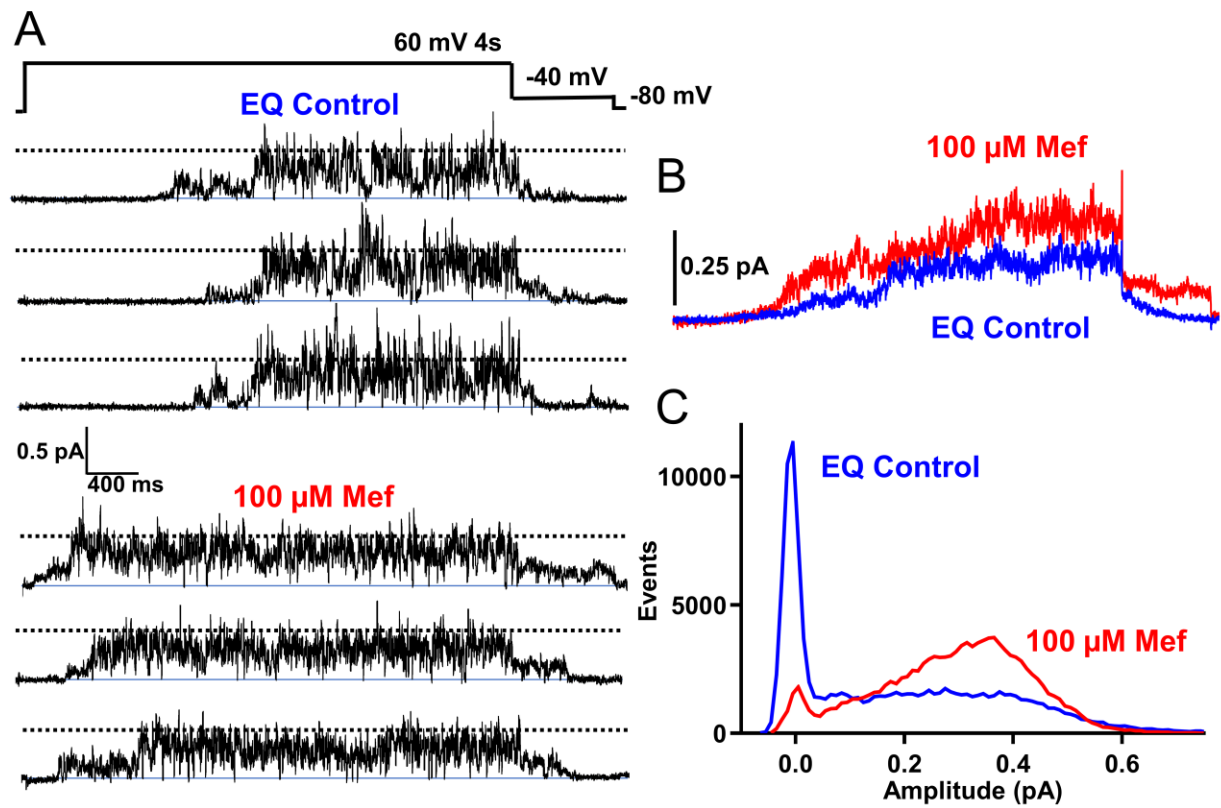
## Figure 4

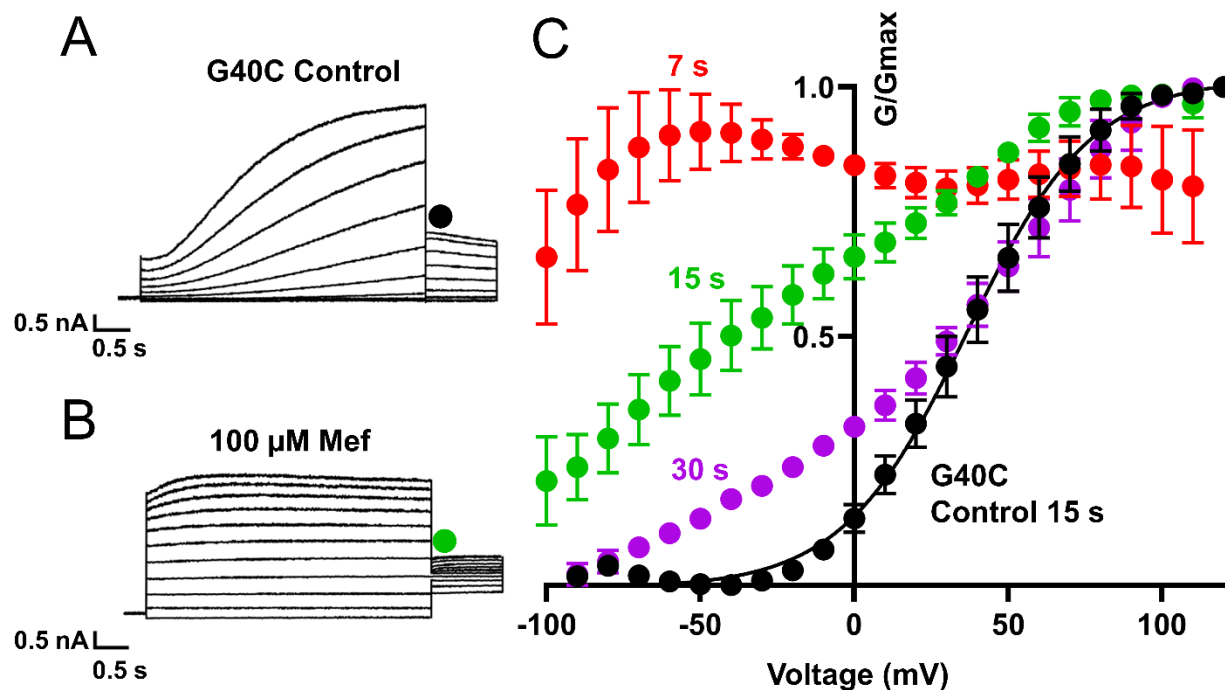# Figure 5

Figure 6

# Figure 7

Figure 8
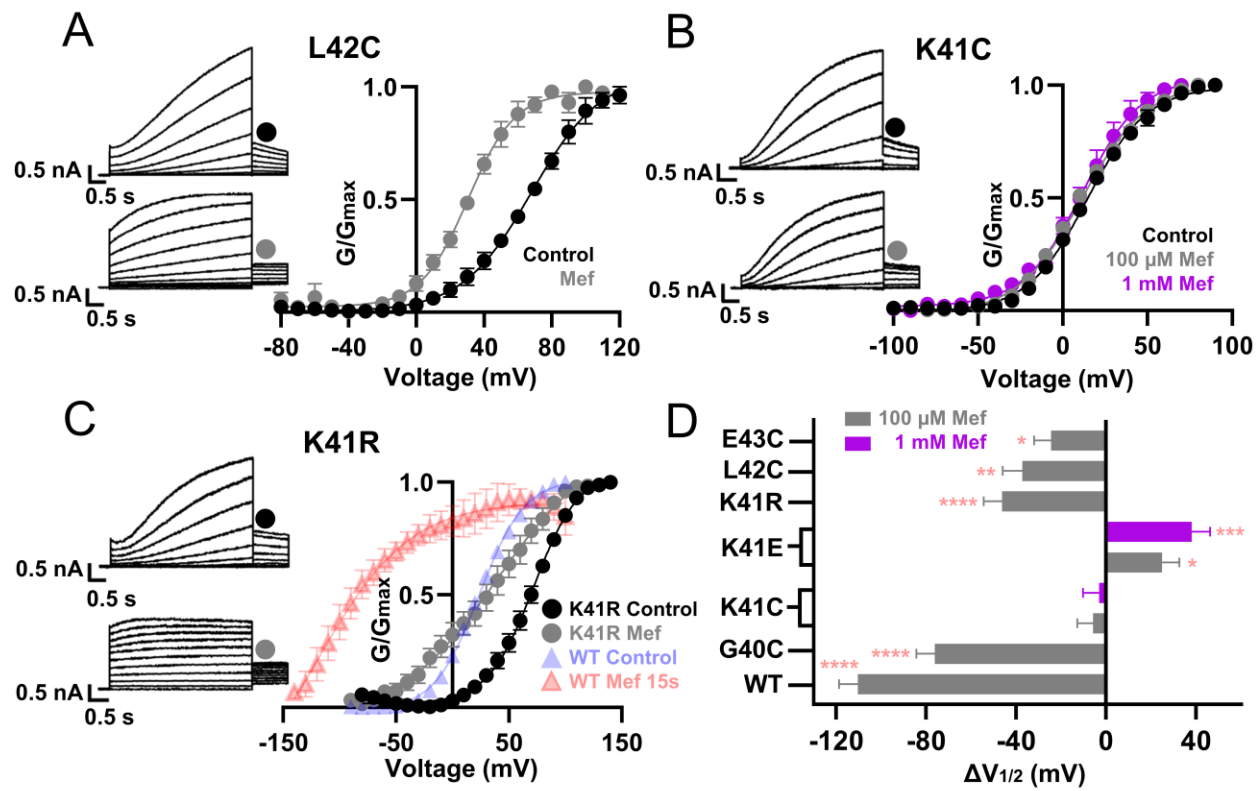
# Supplemental Data

# The $I_{Ks}$ ion channel activator, mefenamic acid, requires KCNE1 and modulates channel gating in a subunit-dependent manner

Yundi Wang, Jodene Eldstrom, and David Fedida[*]

Department of Anesthesiology, Pharmacology and Therapeutics, University of British Columbia, Vancouver, British Columbia, Canada

Keywords: $I_{Ks}$, mefenamic acid, KCNE1, KCNQ1, single channels, gating modifier

**Supplemental Figure 1. Effect of mefenamic acid is preserved in the G40C $I_{Ks}$ mutant.** The currents and conductance-voltage (G-V) plots were obtained using the protocols described in Fig. 3. (A) Currents are shown for G40C in the absence of mefenamic acid (control; interpulse interval was 15 s). (B) Currents are shown for G40C in the presence of 100 µM mefenamic acid (interpulse interval was 15 s). (C) Effect of different interpulse intervals on G-V plots in control and 100 µM mefenamic acid. Intervals were 15 s in control (n = 4; black), and 7 s (n = 3; red), 15 s (n = 3; green) or 30 s (n = 3; purple) in mefenamic acid.